Report on the simulations of a large gas cell with electric field guidance for IGISOL

Heikki Penttilä, Olga Beliuskina, and the IGISOL group

University of Jyväskylä, Department of Physics, P.O. Box 35, FI-40014 Jyväskylä, Finland

Zhihao Gao, Andreas Solders, Ali Al-Adili, Simone Cannarozzo, Mattias Lantz, and Stephan Pomp

Department of Physics and Astronomy, Uppsala University, BOX 516, 75120 Uppsala, Sweden

Introductory note

The aim of the task is to design a large gas stopper with electric field guidance for the IGISOL (Ion Guide Isotope Separation On-Line) mass separation facility in the acceleration laboratory of the Department of Physics of JYU.

In this report the feasibility of the concept is studied, based on experience on similar facilities elsewhere and simulations on the stopping efficiency. These studies are summarized below, and the more detailed description of performed studies can be found in **two attached reports.** The first one (appendix 1) is an internal report of postdoctoral researched Olga Beliuskina, another one (appendix 2) is a manuscript of a proceedings article (https://doi.org/10.1051/epjconf/202328404011) for the 15th Conference of Nuclear Data for Science and Industry, ND-2023, by Zhihao Gao et al..

Summary of results

The largest gas stopper that can be implemented to IGISOL without major modifications in the mass separator front end is 250 mm tall and 400 long in the direction of ion transportation. The available space would allow the width of the gas cell exceed 250 mm, but constructing a device with a cylindrical symmetry is technically beneficial. A 400 mm long gas cylinder with 250 mm diameter was thus used as the basis of simulations.

The key question of the simulations was whether a cryogenic device is needed for sufficient stopping of fission products.

The simulations performed with SRIM and GEANT4 show that almost 50 % of the fission recoils that enter in the stopping gas can be stopped in a room temperature gas cell operated in 400 mbar pressure. This is equal to the highest pressures currently used at IGISOL, and it is known to be manageable.

The improvement factor of fission product stopping with room temperature operation is of the order of 5 for neutron-induced and about 10 for proton-induced fission ion guide. It is thus concluded that *the ion stopping in the non-cryogenic approach is sufficient*, which allows avoiding the technical complications related to installing a cryogenic device in high voltage, high radiation area, as well as in taking account the requirement of the ion guide being easily removable, thus allowing the versatile operation of other ion guide designs.

Although operating in the low temperature has other advantages, those are exceeded by the complications and cost of the cryogenic operation.

The project will proceed towards producing technical drawings of a prototype of a room temperature stopping gas cell with the afore-mentioned dimensions.

Background: Requirements and limitations

The main restrictions for the large gas stopping cell at IGISOL arise from the following.

The gas stopper needs to be **in high radiation area**. While this is true for any large gas stoppers, the environment is in particular challenging, since the accelerated beams are in most cases light ions. In fission experiments that compose more than a half of the experiments run at the IGISOL facility during the latest decade, 30 MeV protons with beam intensities up to several tens of microamperes are the typical ones (50 μA equals ~$3x10^{14}$ protons/s). These intense beams do not only cause radiation during the operation, but they also activate the structures, most pronouncedly beam windows and collimators. Therefore, the access to the IGISOL front end cave, the site of the stopping gas cell, is not limited only during the primary beam irradiation period, but also a significant period after the primary beam has turned off.

The gas stopper needs to be **in high voltage**, which limits means for the remote operation, necessary due to the fact it is also a high radiation area.

The **room** in the area where the gas stopper is to be located **is limited**, largely due to the required radiation shielding.

The **large gas cell should neither limit the divergent use of the IGISOL mass separator target area**. While the large gas cell is most useful for particle induced fission as well as for the multinucleon transfer (MNT), the ion guide technique can be adapted for various other nuclear reactions. There are specific ion guide designs for heavy ion induced fusion, and for light ion induced fusion reactions. These ion guides, which are known to be very reliable, are used in a large fraction of on-line experiments at the IGISOL. In addition, there is a hot cavity ion source that is even more specifically aimed producing ions of just particular elements, for which it provides much faster and more efficient production than any gas cell design. The large gas cell must not prohibit the use of other ion guides. It has therefore to be possible install and remove any kind of ion guide – including the large one – with a reasonable amount of effort. In practice it means that any ion guide, again including the large gas cell, must fit in to the target chamber in the IGISOL front end. Although the target chamber design can be modified, the starting point has been a minimal change to the current one, since the changes in the target chamber can further trigger changes in the design of the existing ion guides and ion sources.

In the planning it is also acknowledged that the length of the **shutdown of the IGISOL facility** operations caused by the commission of a large gas cell **should remain reasonably short, i.e, 2 – 3 months.** The expenses are wanted to keep on acceptable level as well.

Key question: Cryogenic or room temperature operation

A key question behind the performed simulations is the operating temperature of the gas cell.

Operating a gas cell in a low temperature (100 K or below) is beneficial for two reasons.

First, the low temperature improves the stopping efficiency of ions inversely proportionally to the temperature. Second, the low temperature in general reduces losses by chemical and charge exchange reactions since the impurity atoms and molecules (water, oxygen, nitrogen, other noble gases) in the helium buffer gas will be frozen on surfaces.

On the other hand, cryogenic systems are expensive, acquire space and require power, and in general are making the operation of the ion guide more complicated and less reliable. Reaching the lowest temperatures also requires use of cryocoolers, which can be run in high radiation environment if their control units can be in lower radiation environment or sufficiently shielded. However, bearing in mind that the radiation levels in the IGISOL front end increase during operation in such a way that immediate access is not possible, it also means that maintenance or troubleshooting of any instrumentation in the front-end cave that cannot be performed remotely is also out of question after approximately the first two days of experiments.

Results and conclusions

The simulations were based on the available space in the current IGISOL target chamber, i.e., the vacuum chamber housing the ion guide. This chamber is intensively pumped with a Roots blower array to provide differential pumping, whose purpose is to remove the stopping gas before the high vacuum in the acceleration stage of the IGISOL mass separator. The height of the chamber is 258 mm, available space in the primary beam direction >400 mm and <400 mm in the mass separator axis direction.

Simulations (SRIM and GEANT4) were based on cylinder shaped geometry, where the ions would be transported in the direction of cylinder axis with a DC electric field, guided with a RF carpet to the exit nozzle and extracted with gas flow. The diameter of the cylinder was taken as 250 mm and length 400 mm. For neutron induced fission the target was assumed to be placed on the side of the ion guide, for proton induced fission targets would be placed in a channel passing through the ion guide. The geometry for the neutrons is shown below.

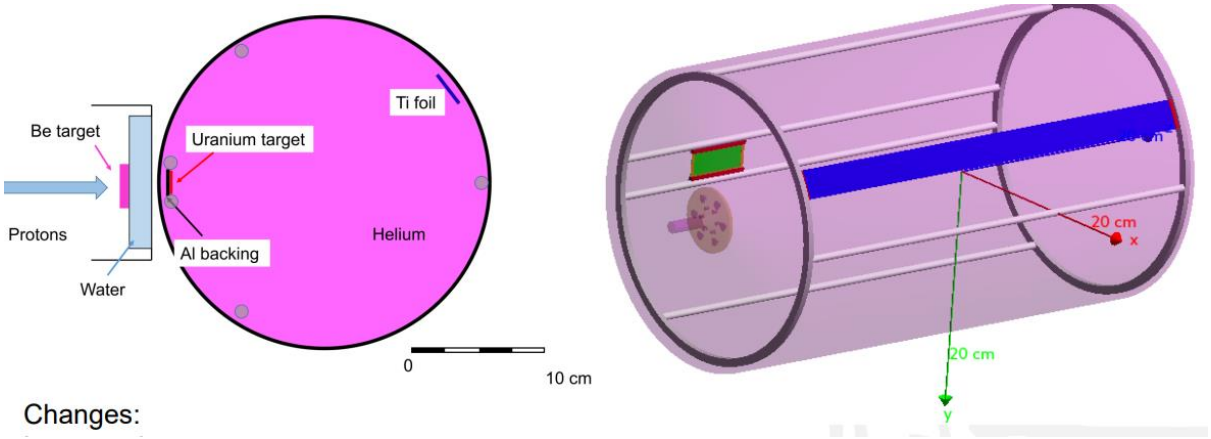

Changes:

In the simulations the stopping gas pressure and temperature was varied between 100 and 400 millibars and 80 K and room temperature 280 K, respectively. The simulations of the stopping efficiency show that 45 % of the fission recoils that enter in the stopping gas can be stopped in a room temperature gas cell operated in 400 mbar pressure. 100 % stopping efficiency would require reducing the temperature to 180 K, with a further reduction to 80 K a pressure of 200 mbar is sufficient to essentially stop all the fission products entering in the gas cell.

Even with the room temperature operation, the improvement factor of fission product stopping is of the order of 5, when compared to the previous neutron induced fission ion guide, and close to 10 for the proton induced fission ion guide. As conclusion, it seems that the room temperature (non-cryogenic) large ion guide would be sufficient. Although operating in the low temperature has other advantages, those are exceeded by the complications and cost of the cryogenic operation.

The project will proceed towards producing technical drawings of a prototype of a room temperature stopping gas cell with the afore-mentioned dimensions.

Appendix 1

Cryogenic Ion Guide for IGISOL (CIGI)

Olga Beliuskina

University of Jyväskylä, Department of Physics, P.O. Box 35, FI-40014 Jyväskylä, Finland

Cryogenic Ion Guide for IGISOL (CIGI)

O. Beliuskina

Introduction

The high ionization potential of the noble gas atoms (such as helium and argon) prevents charge-exchange processes between the ions of interest and the buffer gas atoms resulting in long ion survival times. It is also possible to use high-density gasses for stopping energetic particles. Combining these two aspects does make gas cells an attractive approach to slow down radioactive ions after their production and transport them out of the gas cell to an on-line mass separator. This transport can be through **a gas flow inside the gas cell** and **a supersonic expansion at the exit hole of the cell**. Depending on the dimensions of the cell and on the conductance of the exit hole, transport times will ranges from ms to several seconds. For example, for the stopping volumes of up to 2×10^5 cm^3 [1-4] dictated by the high energies and emittances at in-flight separators, considering practical limits to the gas flow through the exit-hole that can be handled, **gas flow is too slow** for efficient ion extraction of short-lived isotopes. For example, an exit-hole diameter of 1 mm, having a conductance of 0.45 l/s for helium gas at room temperature, combined with this huge stopping volume gives a helium gas refresh rate of once per 7 min (GSI gas catcher an example). In this case **electric-field guidance of the ions is needed** for fast and efficient extraction.

The most common ion guidance **uses a static electric field to push ions towards the exit-hole** side of the stopping volume where the ions encounter an RF electrode structure in the shape of a carpet or a funnel [4,6-8]. The resulting inhomogeneous RF electric field close to the RF electrode structure provides a time-averaged repelling force. **Combining this force with a DC electric field forces** the ions to travel along the RF structure towards the exit hole. Very near the exit hole, the force generated by the gas flow becomes dominant and the ions are swept out of the stopping cell.

The stopping of energetic ions creates **a large number of ion– electron pairs** (one for every 41 eV of energy loss in helium and 26 eV in argon). Ions and electrons move in opposite directions under the influence of the applied DC field. As the electrons have a mobility typically 3 orders of magnitude larger than that of the positive ions, the electron density is the same factor smaller than that of the positive ions; **recombination of the thermalized ions with electrons is thus of no concern.** For a sufficiently large ionization density, the positive ion cloud blows up by **space-charge forces**. In this case, **an RF wall along the body of the cell** can be added **to contain the ion cloud** [8]. If the ionization density is so high as to create a plasma that shields the applied DC field, electrons and ions are not pulled apart and, in addition to the fact that the ions are not transported by the DC field, neutraliza-tion will occur [8-11].

Ions will form undesired molecules/adducts with impurity atoms/molecules. To limit this process to an acceptable level, **a stopping gas impurity concentration better than about 1 ppb is needed** (see e.g. [12]). **Ultra-high-purity stopping cells**, aiming at sub-ppb impurity levels, have been constructed employing ultra-high-vacuum technology (see e.g. [13]). Although possible, this is far from trivial. Earlier works on the ion survival and transport in a closed cell [14-16] has shown that a sufficient purity level can be achieved by in-situ purification of the noble gas upon **cooling the stopping cell to below about 90 K** (**when operating at a density equivalent to 1 bar pressure at room temperature**). The efficiencies measured at low temperature are comparable to those achieved with ultra-high-purity stopping cells at room temperature.

As to summarize mentioned above for a successful performance of the gas cell there are a few problems need to be addressed via building(designing) a new gas cell. To handle the reasonable extraction time and to prevent neutralization of the created products as well as space charge screening the DC and RF needed. Another problem,

mentioned above, is gas impurities which create troubles in dense gasses. Experimentally it was shown that at less than 90 K the impurities are gone.

Existing gas cell overview

Such gas cells are presently in use at different accelerator laboratories, for example: CARIBU at the Argonne National Lab [17], Advanced cryogenic gas stopper at the National Superconducting Cyclotron Laboratory (ACGS) [18], cryogenic gas stopping cell of SHIPTRAP [19] and FRS Ion Catcher at GSI[2,5,15]. In Table 1 there is a summary of main parameters of these cells.

Table 1. Stopping gas cells.

SETUP	Reactions	Energies	Tem-re, K	Pressure, mbar	ρ, $x10^{-5}$ g/cm^3	Volume $x10^5 cm^3$	Length, cm	d_{eff}, mg/cm^2
CARIBU	^{252}Cf FF products	~1 MeV/u	243	50	2.1	0.3	120	2.5
ACGS	Projectile fragmentation	~100 MeV/u	50	40	2.9	2.5	140	5.4
SHIPTRAP	Fusion-evaporation	~1 MeV/u	40/300	7.5/56	0.9	0.56	45	0.4
ION CATCHER	Projectile fragmentation	~100 MeV/u	78/60	47/250	2.9/20.1	0.5	120	5.8/24.1
IGISOL 2010	Projectile fragmentation	~100 MeV/u	96/85	400/50	20.1/2.8	$3x10^{-5}$	3	0.6/0.1
IGISOL future	Proton and neutron induced FFs	~1 MeV/u	90K	200	9.6	0.05	18	1.7

Let us look closer. The actual inner volumes of these gas cells are rather big as of about $0.3x10^5$ cm^3 of the smallest (ACGS) [18] up to 2.5 $x10^5$ cm^3 of the biggest (CARIBU) [17].
The wide range of masses and energies for products of interests: for example, the CARIBU build up for the FPs with the energies of about 1 MeV/u, the SHIPTRAP was designed for very heavy products of fusion-evaporation reactions at energies typically less than 1 MeV/u. From the other hand ACGS and FRS Ion Catcher were designed for the projectile fragmentation products of quite a broad energy range up to few hundreds MeV per nucleon (before the degrader set) with masses up to heaviest projectiles like Uranium. In the end, the final and most clear parameter which was aimed on is the effective thickness of the stopping volume. For example, for the heavy products of interests with the energy up to 10 MeV/u the desired effective thickness is about 20 mg/cm^2. By varying different parameters of the system (such as actual stopping distance, gas temperature and pressure) one can get the desire effective thicknesses: for example, ^{210}Pb with the energy of 10 MeV/u can be efficiently stopped in room temperature He gas at 1 bar pressure in the 120 cm long gas cell.

IGISOL Cryo ion guide first attempt

In order to pursue these studies at the IGISOL and to verify whether primary ions and/or secondary nuclear reaction products can be stopped and extracted from a low temperature gas cell, a cryogenically cooled ion guide, with a small stopping volume of 3 cm^3, was developed at the University of Groningen and tested at the University of Jyväskylä (basic parameters listed in Table 1)[20]. The experiments were carried out by employing

beams from the K-130 cyclotron and the IGISOL 21] technique. The cryogenic ion guide (CIG) was based on the existing light-ion guide design [22]. It was designed for off-line studies with a recoil source (^{223}Ra) and for radioactive species from light-ion induced fusion-evaporation reactions produces on-line. However, the small size (stopping volume length 30 mm) limited the useful stopping range to a fraction of that obtained with a larger volume gas catcher. On the other hand, the small volume provided a fast (few ms) and thus potentially efficient extraction of ions using gas flow alone. In the experiment, 300 and 340 MeV $^{58}Ni^{12+}$ beams from the K-130 cyclotron were degraded in energy, stopped and extracted from the ion guide. Radioactive ion beams were produced by bombard-ing a 4.4 mg/cm^2 ^{nat}Mg target with 40 MeV protons. To test the extraction of radioactive ions under off-line conditions (i.e. with-out cyclotron beam) the aforementioned ^{223}Ra a-recoil source was used. The ion guide and stopping gas were cooled by a custom-built cryostat [23] which was based on a 40 l liquid nitrogen (LN_2) bath with a copper cold finger connected. The whole assembly was mounted vertically onto the IGISOL target chamber such that the light-ion guide was in the same location as it would be using the regular installation through the side of the chamber. The cryostat LN_2 volume had a 7 m spiral copper tube for pre-cooling the He gas before injection into the ion guide via the cold finger. The standard light ion guide (with 0.5 mm diameter exit hole) was mounted onto the tip of the cold finger. A vacuum-tight connection between the insulating vacuum vessel and the ion guide/cryostat was made with a custom-designed thin mylar collar to ensure minimal thermal conductivity.

The lowest achievable temperature measured without a helium gas load was approximately 80 K, reached in about 50 min, and with gas load, the temperature was seen to increase from 85 K to 96 K as the pressure was varied from 50 to 400 mbar (more details see in Ref[24]). This effect can be explained not only by the fact that the ion guide is exposed to the surrounding vacuum chamber, but also to the insufficient pumping arrangements of the cold finger insulating vacuum (due to restrictions placed by the operating environment, the pumping of the insulating vacuum had to be handled with the same pumping system as the target chamber, leading to heat leaks with increasing gas load).

The conductance of the ion guide exit hole (l/s) scales with $T^{1/2}$ and at room temperature (300 K) is calculated to be 0.112 l/s. When the ion guide is operated at 90 K, the conductance decreases to 0.061 l/s. For a volume of 3 cm^3, the evacuation time of the whole guide increases from 27 ms to 49 ms as the temperature reduces from 300 K to 90 K. These results pointed towards a practical advantage of the use of cryogenic gas: for the same helium density, and thus stopping power, the differential pumping requirements are relaxed compared to room temperature operation. Conversely, and important for IGISOL operations, **for the same pumping system a higher stopping gas density can be used**.

One of the **key motivations** for cryogenic operation was **the purification of the catcher gas** from potentially chemically active gases such **as oxygen and nitrogen**, not to mention **water vapor and other water-based molecules and radicals**. To verify the effectiveness of the cryogenic ion guide, mass spectra were measured at room temperature and compared to low temperature (90 K) operation by an MCP at the switch yard of the dipole magnet. The ion guide pressure was adjusted in the two temperature regimes to achieve equivalent helium densities ($\rho_{He} \approx 8x10^{18}$ atoms / cm^3, equal to 0.05 mg/cm^3). The ionization of the helium gas and impurities was caused by the passage of the primary nickel beam prior to optimization of the energy degraders for stopping measurements. The beam intensity was kept at approximately 10^7 pps for both scans.

The effect of freezing out impurities was clearly demonstrated as several mass peaks disappear at low temperature. The majority of mass peaks in the high mass range are likely to be associated with complex molecules and hydrocarbons. The latter is supported by the pattern with a step of 14 mass units (representing CH_2) that is seen in the mass spectra above mass 40.

As the ion guide and helium gas are cooled down, water-based impurities (H_3O^+, $H_5O_2^+$, etc.) are frozen from the gas and the mass peak ratios are strongly suppressed. However, the lowest temperature achievable with this setup is from 80 to 90 K, and therefore oxygen and nitrogen are not frozen from the gas. In fact, the mass peaks at A/q = 14, 16, 28 and 32 (N^+, O^+, N^+_2 and O^+_2) are visibly enhanced. Furthermore, the ion currents of neon (A/q = 20, 22) and argon increase when cooling, whereas xenon is reduced. It is worth commenting on the suspected origin of the nitrogen and oxygen in the mass spectra which could be used as an indicator for an air leak in the system.

The **temperature dependence of molecular formation, recombination, impurities, and charge exchange on the ion survival processes** are an **additional complication**. At low temperature, the enhancement seen in the buffer gas ions and impurity molecules not frozen from the gas is likely to be caused by an overall reduction in the number of charge exchange reactions between the unfrozen species (buffer gas ions, nitrogen, oxygen and so on) and heavier complex molecules and/or hydrocarbons. Th main conclusion was that to **achieve a better suppression of the impurities**, lower **temperatures, below that of LN_2**, should be reached. The most practical way to achieve this would be **the use of a cryocooler instead of a cryogenic liquid bath**.

Fission products

Independent fission product yields are an important characteristic of nuclear fission and better knowledge of how the yield distributions varies with fissioning system will improve our understanding of the fission process. For energy applications fission yield data are important in criticality and reactivity calculations for reactor design, dosimetry and fission gas production for reactor safety and for improved burn-up predictions.
At the IGISOL, typically independent fission product yields have been measured for proton induced fission of ^{nat}U. Fission is induced in a target situated in a helium gas filled ion guide. Through collisions with the helium gas the highly-ionized high-energy fission products are recombined to form singly charged ions and are brought to rest. A helium gas flow, in combination with a series of electrostatic electrodes, are used to extract the products from the ion guide. Using a dipole magnet, a single isobaric chain is selected and transported to the Penning trap, JYFLTRAP. With this method independent fission yields can be measured through direct ion counting just a few hundred milliseconds after fission [25-28].
For nuclear energy applications another process, neutron induced fission, is of main interest. Moreover, neutron induced fission also produces more neutron rich products, of interest in the studies of nuclides far from the line of stability. To facilitate this reaction at IGISOL a Be(p,xn) neutron converter and a dedicated ion guide for neutron Induced fission has been developed [29-31].

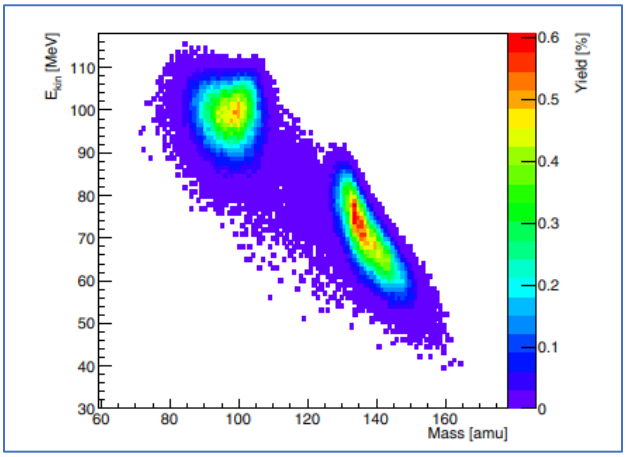

Figure 1. Simulation of fission fragment yields of ^{238}U(n,f) at E_n = 4 MeV as a function of fragment kinetic energy and mass [26].

Proton and neutron induced fission products are produced in a wide range of nuclides with atomic mass numbers ranging from 70 to 160. In addition, fragments show a large spread in kinetic energy, from 0.3 to 1.2 MeV/u. Figure 1 presents simulation of fission fragment yields of ^{238}U(n,f) at E_n = 4 MeV as a function of fragment kinetic energy and mass.

SRIM simulations

Based on the SRIM simulations one can estimate what are the geometry requirements for the products of interest. First, let's assume ^{100}Tc with the energy of 100 MeV was created at the middle of the ^{238}U target of 15 mg/cm^2. It needs to travel inside the half of the target before entering the buffer gas and it will lose 85% of its energy in the target. At the room temperature of 293 K the remaining kinetic energy of about 15 MeV will allow ^{100}Tc to travel for about 45 cm more in the He gas at 0.1 bar pressure or about 10 cm in the He gas at 0.5 bar pressure before it stops. A bit longer stopping pass will be allowed for ^{100}Tc which was created at the surface of the target and kept all its kinetic energy of 100 MeV before entering the buffer gas. For example, it will be stopped after 123 cm only at 0.1 bar He gas pressure or 25 cm at 0.5 bar He gas pressure. In Table 2 Stopping ranges versus buffer gas pressure listed for both cases of ^{100}Tc created in the middle and at the surface of the ^{238}U target.

Table 2. List of stopping ranges for ^{100}Tc at the room temperature.

Pressure, mbar	Stopping range, cm ^{100}Tc created at the middle of the ^{238}U of 15 mg/cm^2 (Remained energy is 15 MeV), room temperature 293 K	Stopping range, cm ^{100}Tc created at the surface of the ^{238}U of 15 mg/cm^2 (Assuming full energy is 100 MeV), room temperature 293 K
100	45	123
200	25	62
300	15	41
400	11	31
500	9	25

Geometry of the target chamber

Based on the current target chamber geometry there are limitations on the cryogenic-possible-to-be gas cell dimensions. For the maximum outer "cryo chamber" possible diameter (limited by the height of the target chamber) is 25.8 cm. The maximum stopping length depends on the direction of the FP path, which, in its turn, depends on reaction type (target placements): proton-induced or neutron-induced fission or for both cases.

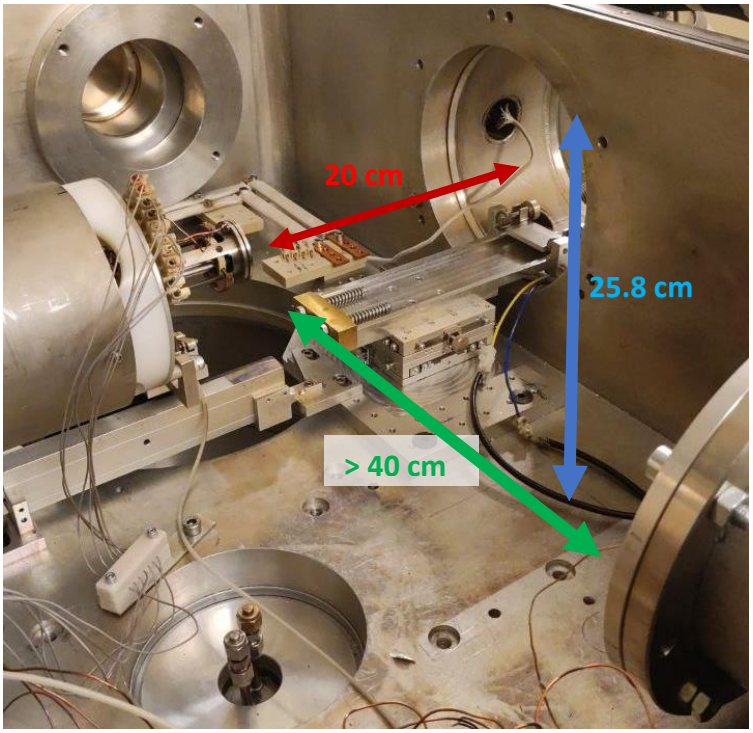

Figure 2. Photo of the target chamber. "Free" space available: target chamber height is 260 cm, about 20 cm from the beam exes to the SPIG, distance from the beam collimator to the "SPIG"-Axis

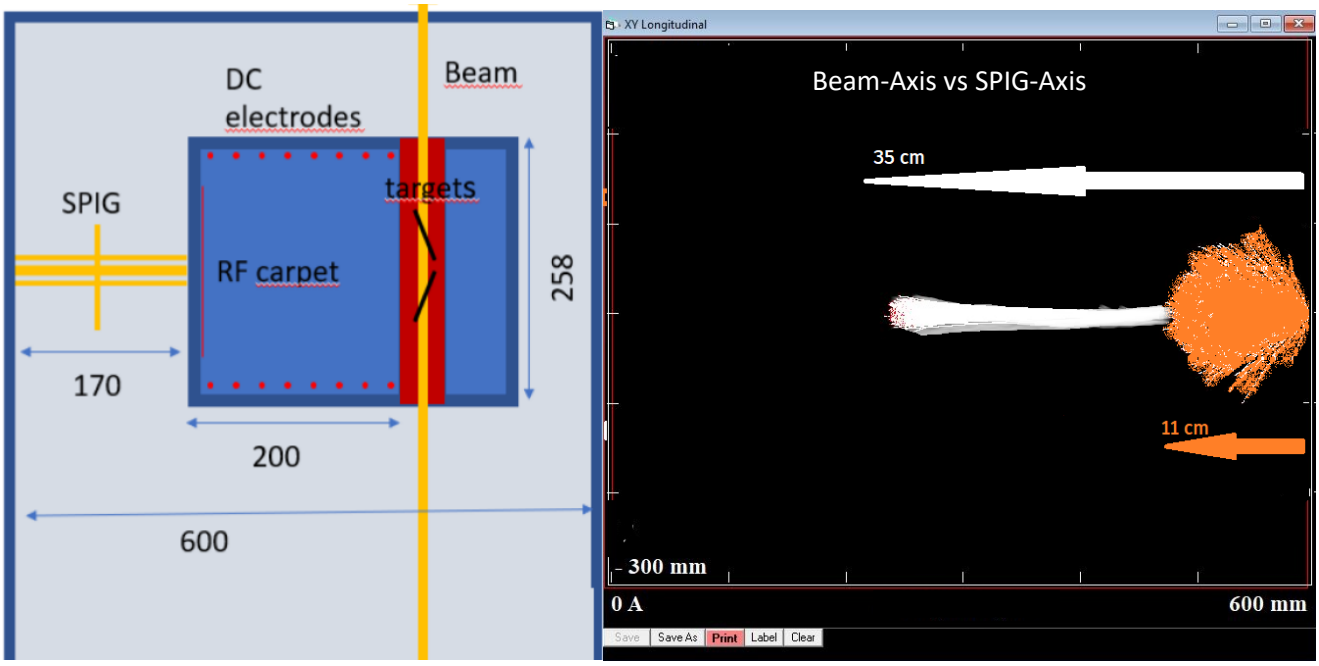

Figure 3. Gas cell placement for proton induced fission and SRIM simulation for cases described in Table 2.

In Figures 3 and 4 the gas cell placements for proton and neutron induced fission are presented. Figure 3 is for the proton induced fission products. It has a beam tube going through the gas cell. This rectangular tube has 2 targets inside (potentially can be more if beneficial). Rectangular, because it would make it easier to attach windows for fission product to fly from target enclosure to the gas cell. Both sides of the window are naturally in the same pressure. The helium in the target volume is partly also for cooling the targets. The FP stopping pass is towards a RF carpet. Without serious target chamber modification, the maximum possible stopping length is about 18 cm. SRIM simulations showed that FP's ranges at the room temperature and the reasonable pressure are longer that the maximum available stopping length. In Table 3 there are results of the SRIM simulations for the stopping ranges of ^{100}Tc at the 100 K temperature.

Table 3. List of stopping ranges for ^{100}Tc at the temperature of 100 K.

Pressure, mbar	Stopping range, cm ^{100}Tc created at the middle of the ^{238}U of 15 mg/cm^2 (Remained energy is 15 MeV), temperature of 100 K	Stopping range, cm ^{100}Tc created at the surface of the ^{238}U of 15 mg/cm^2 (Assuming full energy is 100 MeV), temperature of 100 K
100	15	42
200	7	21
300	5	14
400	4	10
500	3	8

As we can see from Table 3 cooling the buffer gas will allow to increase the stopping efficiency of the gas cell. At 100 K almost all the FP can be stopped.

Figure 4 shows possible placement of the gas cell for the neutron induced fission. Proton-to-neutron converter is outside of the gas cell. Target position is almost on the wall (as close as possible). New simulations showed that

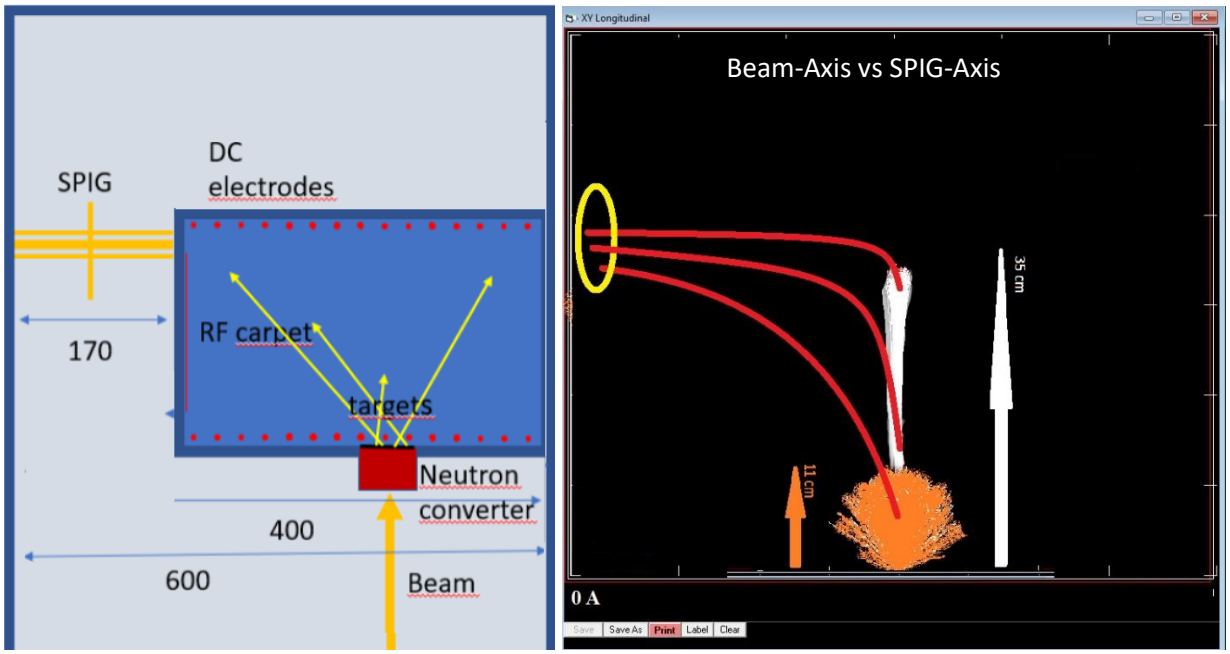

Figure 4. Gas cell placement for neutron induced fission and SRIM simulation for cases described in Table 2.

positioning U targets closer to the p-to-n converter increases the FP production rate. The gas cell length on the direction along with the beam exes so to say “stopping path” is much longer, FPs will be guided to the exit nozzle with the electric field. Although there is a need to simulate rather not trivial electrodes configurations since the FP trajectories vary depending on their initial energy and the place in the target where they were created. In this case position of the cell nozzle will not be symmetrical relating to the cell edges. Here, a second point needs to be addressed is a gas flow and to design gas outlets in such a way that FP which were stopped just after escaping the target will not be lost.
Such configuration does not require cooling the buffer gas to benefit from shorter stopping ranges. The actual stopping distance of such gas cell might be already sufficient.

Simulations

Systematic effects in fission yield measurements due to differences in the stopping efficiencies of the fission fragments were studied in [29] for the neutron induced fission using neutron convertor. Figure 5 presents a cross sectional view of the neutron converter and ion guide of the MCNPX model [32]. The proton beam enters from left. The beryllium disc is indicated in green with the cooling water behind. The Uranium targets are mounted in a holder close to the wall of the ion guide, facing the neutron converter. The recorded neutron flux in the ion guide is displayed in color scale.

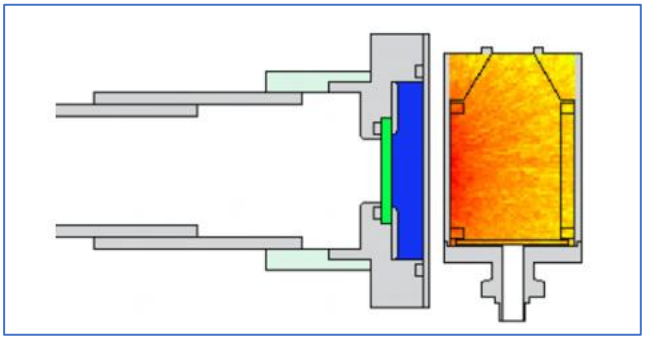

Figure 5. Cross sectional view of the neutron converter and ion guide of the MCNPX model (See details in the text. Simulations are taken from [29]).

Created in [29] framework of the neutron converter and ion guide from the incoming proton beam to the extracted fission products showed nice results which can be used to optimize the geometry with respect to production rate, while at the same time minimizing systematic effects. A combination of different Monte Carlo codes have been used. The production of neutrons in the Be(p,xn) converter was simulated using MCNPX 2.5.0 [32] and the neutron field in the volume occupied by the ion guide was extracted. The neutron induced fission process, including multi chance fission, was handled by the GEF code while a Geant4 model was developed for the transportation and stopping of fission products in the ion guide. Finally, the multiphysics code COMSOL was used to study the evacuation of fission products from the ion guide. For the MCNPX model: a 30 MeV proton beam is impinged on the 5 mm thick beryllium target. Geant4 is used to simulate the stopping of fission products in the helium gas (assuming the FPs loose most of their energy already in the uranium target, before entering the helium gas). For the COMSOL the nominal inlet helium pressure is set to 200 mbar at room temperature while the target chamber, on the other side of a 1.2 mm outlet aperture, is at vacuum.

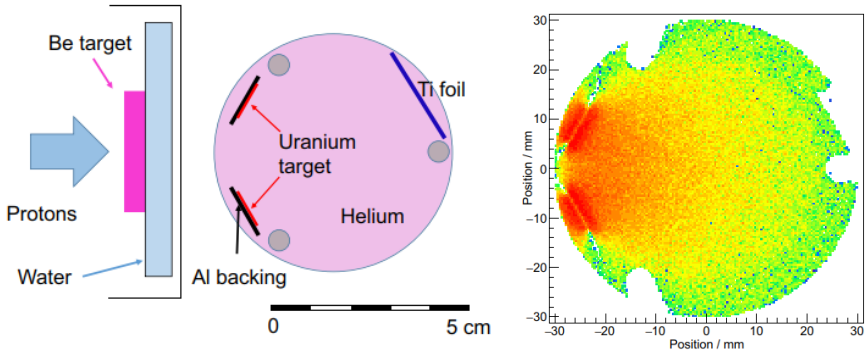

Figure 6. Left figure shows a schematic view of the experimental setup. Stopping of the fission product 112Rh in the ion guide, the right figure shows ions that have come to a stop in the helium gas. This figure is a projection onto the xy-plane.

From the MCNPX simulation the **average neutron flux** in the **two targets** is **2.2x10^9 neutrons per second at 1 µA** proton beam. This will result in a total fission rate of **5.5x10^5 fissions per second** using **two standard** IGISOL targets of **10 mm by 50 mm at a thickness of 14 mg/cm^2.**
As an example, the full simulation has only been completed for a few fission products for ^{112}Rh. In Fig. 6 the result for ^{112}Rh is presented. The right part of Fig. 6 shows the final position of the ions that stop in the gas. Most of the ions that end up in the gas are stopped close to the uranium targets. The total number of ^{112}Rh ions stopped in the gas is 24 per second at a proton beam current of 1 µA, which amounts to about 2.3% of the total number of ^{112}Rh produced in the targets. The COMSOL result shows that the helium flow is sufficient to extract about 15% of the ions and the average extraction time of those that get out is 113 ms.

The count rate of mass separated ^{112}Rh ions after the dipole magnet estimated to be as low as one, or a few, per second at 1 μA proton beam current. In proton-induced fission, count rates of several thousand ^{112}Rh per second can be obtained, however, the yield of ^{112}Rh is about ten times higher in proton induced fission compared to the neutron induced case. As to say there are 2 orders of magnitude in the count rate lost. Based on these values one can conclude that there is a need in increasing the stopping + extraction efficiency of the fission ion guide.

GIANT4 Simulations

Considering studies above GIANT4 simulations were performed to compare stopping efficiency obtained in [26-29] with expected stopping efficiency adopted new gas cell geometry at room temperature and at 80 K (temperature at which all the impurities of the buffer gas expected to freeze out). Table 3 lists results of these simulations for four different configurations + condition of the gas cell. **V1:** the He gas temperature is 293 K at the pressure of 400 mbar, the gas cell diameter is Ø = 6 cm, the stopping distance l = 7 cm. **V2:** the He gas temperature is 280 K at the pressure of 400 mbar, the gas cell diameter is Ø = 25 cm, the stopping distance l = 40 cm. **V3:** the He gas temperature is 80 K at the pressure of 400 mbar, the gas cell diameter is Ø = 25 cm, the stopping distance l = 40 cm. And finally, **V4:** the He gas temperature is 80 K at the pressure of 115 mbar, the gas cell diameter is Ø = 25 cm, the stopping distance l = 40 cm.
In the V1 conditions two Uranium targets of 14 mg/cm^2 were used and about 70% of FP is stopped inside the targets. For V2, V3 and V4 sets two Uranium targets were used of 15 mg/cm^2 thicknesses and 72% of FP never left targets.
For the very short stopping length of 7 cm in He gas at room temperature and 400 mbar pressure only about 1% of FP were stopped. As expected, the increasing gas cell dimensions leads to an increase in the stopping efficiency

as well, for example for the conditions V2 with 40 cm of the stopping path about one order of magnitude. Cooling down the He gas to 80 K gives additional boost in the stopping efficiency, but not that tremendous.

Table 3. The fraction of fission products stopped in U targets and in the Helium gas.

	V1	V2	V3	V4
	293 K, 400 mbar Ø = 6 cm, l = 7 cm	280 K, 400 mbar Ø = 25 cm, l = 40 cm	80 K, 400 mbar Ø = 25 cm, l = 40 cm	80 K, 115 mbar Ø = 25 cm, l = 40 cm
Uranium targets	70%	72%	72%	72%
Helium gas	0.87%	9%	12%	9%

Conclusion

Considering current target chamber geometry and results of the performed simulation:

1. For the proton-induced fission the cryogenic gas cell recommended.
2. For the neutron induced fission at the room temperature the higher stopping efficiency can be achieved at higher buffer gas pressure.
3. Some increase in the final count rate can be reached via using a bit thinner target that more FP will escape from targets and will be stopped and extracted from the gas cell.

References

1. M. Petrick, et al., NIM B 266 (2008) 4493.
2. M. Ranjan, et al., Europhysics Letters 96 (2011) 52001.
3. M. Wada, et al., NIM B 204 (2003) 570.
4. L. Weissman, et al., NIM A 540 (2005) 245.
5. M. Ranjan, el al., NIM A 770 (2015) 87.
6. G. Savard, et al., NIM B 204 (2003) 582.
7. I. Katayama, et al., Hyperfine Interactions 115 (1998) 165.
8. A. Takamine, et al., Review of Scientific Instruments 76 (2005) 103503.
9. S. Palestini, et al., NIM A 421 (1999) 75.
10. M. Huyse, et al., NIM B 187 (2002) 535.
11. M. Facina, G. Bollen, D. Morrissey, Hyperfine Interactions 174 (2007) 21.
12. Y. Kudryavtsev, et al., NIM B 179 (2001) 412.
13. G. Savard, et al., NIM B 204 (2003) 582.
14. P. Dendooven, S. Purushothaman, K. Gloos, NIM A 558 (2006) 580.
15. S. Purushothaman, Superfluid Helium and Cryogenic Noble gases as Stopping Media (Ph.D. thesis), KVI, University of Groningen, Groningen, Netherlands, 2008.
16. S. Purushothaman, et al., NIM B 266 (2008) 4488.
17. G. Savard, A.F. Levand, B.J. Zabransky, NIM B 376 (2016) 246.
18. R. Ringl, et al., NIM B 496 (2021) 61.
19. C. Droese, et al., NIM B 338 (2014) 126.
20. A. Saastamoinen, el al, NIM A 685 (2012) 70.
21. J.Äystö, Nuclear Physics A 693 (2001) 477.

22. J. Huikari, et al., NIM B 222 (2004) 632.
23. B.V. Vacuum Specials, Woerden, The Netherlands /http://www.vacuumspecials.nl/S.
24. M. Ranjan, Ph.D. Thesis, University of Groningen, 2012.
25. V. Rakopoulos, el al., EPJ Web of Conferences 146 (2017) 04054.
26. A. Solders, el al., EPJ Web of Conferences 146 (2017) 03025.
27. S. Pomp, el al., EPJ Web of Conferences 169 (2018) 00017.
28. Z. Gao, el al., EPJ Web of Conferences 239 (2020) 17019.
29. A. Solders, et al., Nuclear Data Sheets 119 (2014) 338.
30. A. Mattera, et al., Nuclear Data Sheets 119 (2014) 416.
31. D. Gorelov, et al., NIM B 376 (2016) 46.
32. D.B. Pelowitz, Ed., MCNPX Users Manual Version 2.5.0'', LA-CP-05-0369 (2005)

Appendix 2

New design and simulation of the ion guide for neutron-induced fission products at the IGISOL facility

Zhihao Gao, Andreas Solders, Ali Al-Adili, Simone Cannarozzo, Mattias Lantz, Heikki Penttilä*, Stephan Pomp, and the IGISOL team*

Department of Physics and Astronomy, Uppsala University, BOX 516, 75120 Uppsala, Sweden

*Department of Physics, University of Jyväskylä, P.O.Box 35, FI-40014 Jyväskylä, Finland

New design and simulation of the ion guide for neutron-induced fission products at the IGISOL facility

Zhihao Gao[1,*], *Andreas* Solders[1,**], *Ali* Al-Adili[1], *Simone* Cannarozzo[1], *Mattias* Lantz[1], *Heikki* Penttilä[2], *Stephan* Pomp[1], and *the IGISOL* team[2]

[1]Department of Physics and Astronomy, Uppsala University, BOX 516, 75120 Uppsala, Sweden
[2]Department of Physics, FI-40014 University of Jyväskylä, Finland

Abstract. Measurements of independent fission yield distributions in neutron-induced fission at high neutron energies are important for our fundamental understanding of the fission process, and are also relevant for reactor physics applications. So far, measurements of independent fission yields in proton-induced fission have been performed at the IGISOL facility at the University of Jyväskylä, using the Penning trap as a high resolving-power mass-filter. In order to also facilitate measurements of neutron-induced fission, a dedicated ion guide and a proton-to-neutron converter was developed. However, the first measurement indicates that fewer fission products than expected reach the Penning trap. To explore potential reasons and possible improvements, a simulation model was also developed and benchmarked. The benchmark showed that the model is able to reproduce the performance of the ion guide remarkably well and that the main reason for the low yield of fission products is the low collection efficiency of the ion guide.
Based on the benchmark, a new ion guide is being designed. In the new design, the positions of the uranium targets and volume of the ion guide have been changed to increase the collection of fission products. This results in a five-fold increase of the yield. However, the collection efficiency of the new ion guide still needs to be improved in order to achieve intensities of the extracted fission products that are large enough to allow for reasonable measurement times.
Because the volume of the ion guide is increased significantly, the extraction time of the ions is expected to be longer than that from the previous ion guide. Therefore, an electric field guidance system that consists of a combination of a stationary electric field and an RF-carpet is considered to be deployed. The stationary field, produced from a set of DC-ring electrodes, accelerates the ions towards the RF-carpet at end plate of the ion guide. The RF-carpet consists of a time-dependent field, produced from a radio-frequent structure of concentric rings, with a DC-component that guides the ions towards the exit hole in the center of the end plate. In this paper we present the current status of the simulations and design of the new ion guide.

1 Introduction

Independent fission yield distributions are a basic observable and are important in the understanding and modeling of the fission process. However, experimental data of complete independent yield distributions are scarce [1]. To facilitate measurements of the independent yields in neutron-induced fission at the Ion Guide Isotope Separator On-Line (IGISOL) facility, a proton-to-neutron converter (*pn*-converter) and a dedicated ion guide was developed and tested [2, 3]. In parallel, a multi-physics Monte Carlo simulation model for the ion guide was developed [4, 5] and benchmarked against γ-spectroscopy data [6]. According to the benchmark, only a small fraction of the fission products, about 0.9%, are stopped in the ion guide.

In the present work, with the aim of increasing the amount of extracted fission products, a new design of the ion guide is presented together with simulations of the system. The geometry of the ion guide, as well as the positions of the targets and the pressure and temperature of the helium gas, are different from those of the previous ion guide [6]. As the density of the helium gas is dependent on the temperature, the impact of the temperature on the collection efficiency is also studied.

To further increase the collection efficiency, as well as to reduce the extraction time of the fission products, an electric guidance system is implemented in the new design. This is inspired by the RF-system used in the CARIBU gas catcher [7] and the cryogenic stopping cell at GSI [8]. The guidance system, including a stationary electric field and a radio frequency field, has been calculated using the software COMSOL [9]. Under the electric guidance, trajectories of the charged ions in the ion guide are simulated with COMSOL. However, these simulations don't take the effect of the helium gas into account.

*e-mail: zhihao.gao@physics.uu.se
**e-mail: andreas.solders@physics.uu.se

2 New designand simulation

2.1 Simulation

Figure 1 shows an optional new design of the ion guide. In the simulation, the physics models and analysis procedures are the same as in the simulations of the previous ion guide [6]. However, in this new design, the diameter is increased from 60 mm to 250 mm and the length of the ion guide is increased from 70 mm to 300 mm. The dimensions are limited by the size of the IGISOL reaction chamber that is used to hold the ion guide. Two uranium targets of the same size as those used with the previous ion guide are used in the present simulation but their positions are changed in order to be closer to the *pn*-converter.

The pressure of the helium gas in the ion guide is reduced from 400 mbar to 150 mbar to eliminate the risk of sparking due to the electric field. The nominal temperature of the helium gas in the simulation is 260 K, which is considered the lowest temperature available without insulating the ion guide. To study the effect of the helium density on the stopping efficiency, different helium temperatures are compared. Results of the simulations with different parameters are presented in section 3.

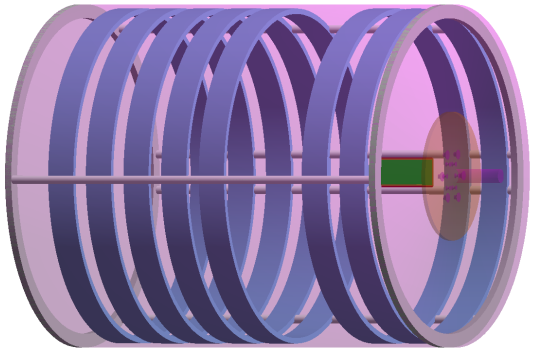

Figure 1. Geometry of the new design of the ion guide in the GEANT4 model. Green: uranium targets. Purple: Helium gas. Blue: DC cage. Red: Aluminum holders.

2.2 Electric fields

The AC/DC Module of COMSOL [9] is used to calculate the electric fields that will be implemented in the GEANT4 model. Figure 2 shows the obtained stationary field from the axial DC-ring electrodes, where the rings are drawn in wire frames to be able to see the electric field. The voltages of the rings from right to left are 5, 4.5, 3.5, 3, 2.5, 2 and 1.5 kV. There is a gap in between the second and third DC-ring, and a corresponding step in the voltages, in order to allow space for the uranium targets. In addition to the seven DC-rings, ten concentric ring electrodes at the end plate (to the left in Figure 2) of the ion guide provide a repellent electric field to prevent the ions from hitting the exit wall.

In Figure 2, the electric field lines are drawn and the field strength is represented by the colors shown in the legend. The electric field strength is around 1.5×10^4 V/m. Later on these parameters will be optimized with respect to the collection efficiency of ions at the end of the ion guide.

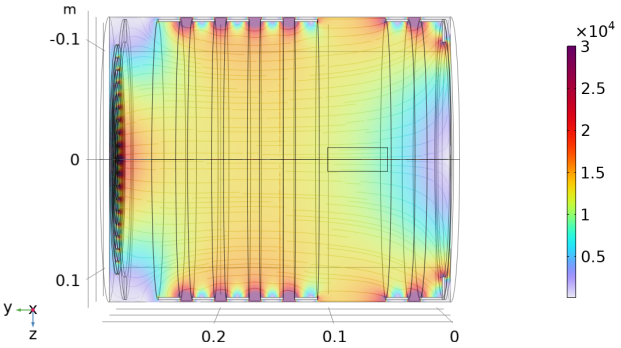

Figure 2. The calculated stationary electric field provided from the DC-rings and the concentric rings at the end plate in the ion guide by COMSOL. Colors represent the field strength in V/m.

The electric field is designed to center the ions on the axis of the ion guide and accelerate them towards the exit. As an example, Figure 3 shows the trajectories of ions with mass number A=100 and ionic charge state +1 obtained with COMSOL. In this calculation the ions are emitted from the surface of the uranium target with an initial energy of 100 eV. These initial conditions correspond to a scenario where the ions, due to energy straggling, has lost most of their energy inside the target. The colors of the legend in Figure 3 show the velocities of the ions in m/s. Disregarding the helium gas, the ions arrive at the end plate of the ion guide in 5 μs and with kinetic energy at the keV scale. Compared to the previous ion guide, where the transport of the ions only relied on the flow of the helium gas, this corresponds to a reduction in the drifting time of several orders of magnitude, as expected. However, the COMSOL simulation disregards the effect of the helium gas, which is expected to increase the collection efficiency as well as the extraction time. In order to take the effect of the helium into account the electric fields will later be imported into the GEANT4 model.

The ions that arrive at the end plate after the transportation in the stationary field are assumed to have a very low energy because of the collisions with the helium gas. Figure 4 shows the geometry of the RF-carpet that consists of a RF-structure and the ten concentric ring electrodes (the rings at the end plate presented in Figure 3). The RF-structure has 200 rings with a width of 250 μm, to which an oscillatory potential at a frequency of 6.25 MHz, with a phase shift of π radians between consecutive electrodes, is applied. In addition, the ten ring electrodes at the end plate, having voltages 1.5 kV to 0.96 kV, provide a stationary field with a gradient towards the center hole. Near the RF-carpet, the transportation of ions is dominated by the combined fields which produces a time average force that transports the ions to the center exit hole. In Figure 4, the

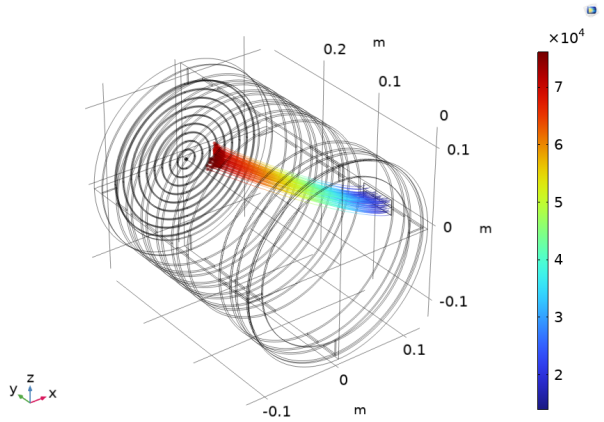

Figure 3. COMSOL: The trajectories of the charged ions in the stationary field during the first 5 μs, disregarding the helium gas. The colors indicate the velocities of ions in m/s.

trajectories shown are those of ions generated on a surface, 10 mm in front of the RF-carpet, at an energy of 0.5 eV. The ions are driven by the combined fields towards the exit hole, in the center of the end plate. However, in this simplified COMSOL model the helium gas is disregarded, which results in an acceleration of the ions instead of a slow mobility.

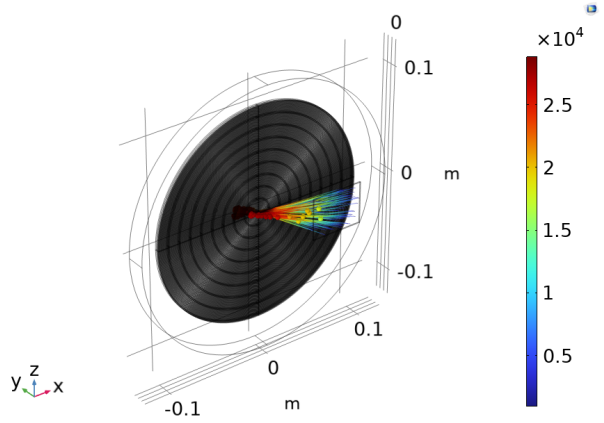

Figure 4. COMSOL simulation: The trajectories of the charged ions in the combined fields near the RF-carpet during the first 6 μs, disregarding the helium gas. The colors indicate the velocities of ions in m/s.

3 Results and discussion

The amount of fission products generated from the uranium targets per second and the amount of fission products stopped in the gas are listed in Table 1, together with the simulation results of the previous ion guide [6]. Compared with those results, 1.2 times more fission products are generated in the uranium targets since the targets are closer to the *pn*-converter. In the simulation with a gas temperature of 260 K and a gas pressure of 150 mbar, the amount of fission products stopped in the gas is increased by a factor of 5 compared to the results of the previous ion guide. The main reason for the increase is the larger volume of gas.

Table 1. Comparisons of the results from the simulations of the previous ion guide and the new design. The factor is the amount of FPs from the present simulation over the amount of FPs from the previous simulation.

	Temperature	Previous ion guide [6]	Present work	Factor
Amount of FPs	260 K	9.36×10^6	1.10×10^7	1.2
Stopping in the gas	260 K	8.10×10^4	4.07×10^5	5.0
Amount of FPs	220 K		1.10×10^7	1.2
Stopping in the gas	220 K		4.94×10^5	6.1
Amount of FPs	180 K		1.10×10^7	1.2
Stopping in the gas	180 K		6.10×10^5	7.5

By decreasing the temperature, as shown in Table 1, more fission products are stopped in the gas. This makes sense since the density of the helium gas increases with the decrease in temperature. However, to achieve temperatures below 260 K, such as 180 K, a cryogenic system would have to be developed. Such a system would make the operation of the ion guide more complex. At the same time, it would reduce the stopping volume of the ion guide due to the necessity of having double walls for insulation. Hence, further investigations are needed to evaluate the benefits of implementing such a system.

4 Outlook

The development of the simulation model is ongoing and the next step will be to implement the electric fields derived from COMSOL into the GEANT4 model. The effect of the helium gas on the transport of the ions in the field has to be included. Furthermore, the RF-carpet will be implemented in the model to simulate the transportation of the ions to the exit hole of the ion guide. The final step will be to optimize all of the parameters concerning the collection of fission products at the exit hole.

Also the influence of size and position of the uranium targets needs to be further investigated. On one hand the uranium targets should be positioned as close as possible to the *pn*-converter, on the other hand it has to be placed to optimize the stopping of the fission products. Further more, if cryogenic temperatures are to be implemented the necessity of having a double wall chamber will pose constraints on the minimum achievable distance between the converter and the target.

5 Acknowledgements

The computations were enabled by resources provided by the Swedish National Infrastructure for Computing (SNIC) at Uppmax partially funded by the Swedish Research Council through grant agreement no. 2018-05973.

This work was supported by the Swedish research council Vetenskapsrådet (Ref. No. 2017-06481), the European Commission within the Horizon 2020 Framework Programme through Fission-2019-SANDA (Project No. 847552), the Swedish Radiation Safety Authority (SSM), and the Swedish Nuclear Fuel and Waste Management Co. (SKB).

References

[1] H. O. Denschag *et al.*, *Compilation and Evaluation of fission Yield Nuclear Data*, (INTERNATIONAL ATOMIC ENERGY AGENCY, Vienna, 2000) 1168

[2] D. Gorelov *et al.*, Nucl. Instrum. Methods Phys. Res. B **376**, 46 (2016)

[3] A. Mattera *et al.*, Eur. Phys. J. A **53**, 173 (2017)

[4] A. Al-Adili *et al.*, Eur. Phys. J. A **51**, 59 (2015)

[5] K. Jansson *et al.*, Eur. Phys. J. A **53**, 243 (2017)

[6] Z. Gao *et al.*, Eur. Phys. J. A **58**, 27 (2022)

[7] G. Savard *et al.*, Nucl. Instrum. Methods Phys. Res. B **376**, 246 (2016)

[8] M. Ranjan *et al.*, Nucl. Instrum. Methods Phys. Res. A **770**, 87 (2016)

[9] *AC/DCModule User's Guide*, (COMSOL AB, Stockholm, Sweden. 2021) 82

[10] T. Eronen *et al.*, Eur. Phys. J. A **48**, 46 (2012)